Available online at www.sciencedirect.com
SCIENCE DIRECT
Journal of Photochemistry and Photobiology A: Chemistry 181 (2006) 306–313
Journal of Photochemistry and Photobiology A:Chemistry
www.elsevier.com/locate/jphotochem

Chemical bath deposited CdS/CdSe-sensitized porous TiO_2 solar cells

Olivia Niitsoo [1], Shaibal K. Sarkar [1], Christophe Pejoux, Sven Rühle [2], David Cahen, Gary Hodes *

Department of Materials and Interfaces, Weizmann Institute of Science, Rehovot 76100, Israel

Received 19 September 2005; received in revised form 13 December 2005; accepted 14 December 2005
Available online 20 January 2006

Abstract

CdSe is homogeneously deposited into nanoporous TiO_2 films and used in liquid junction photoelectrochemical solar cells. The effect of the deposition parameters on the cell are studied, in particular differences between ion-by-ion and cluster deposition mechanisms. CdSe deposition on a Cd-rich CdS film that was deposited first into the TiO_2 film, or selenization of the Cd-rich CdS layer with selenosulphate solution improves the cell parameters. Photocurrent spectral response measurements indicate photocurrent losses due to poor collection efficiencies, as shown by the strong spectral dependence on illumination intensity. Cell efficiencies up to 2.8% under solar conditions have been obtained.

Keywords: Nanoporous solar cell; Chemical bath deposition; CdS; CdSe; TiO_2

1. Introduction

Dye-sensitized nanocrystalline solar cells (DSSC) are a promising alternative to conventional p–n junction solar cells [1]. The advantage of DSSCs over other types of photovoltaic cells is the relative simplicity of their assembly. In the laboratory DSSCs can reach solar-to-electric conversion efficiencies of up to 11%. The conventional DSSC is made from a mesoporous TiO_2 film with adsorbed organo-ruthenium dye molecules acting as light harvester.

Another, relatively less-studied, version uses a nanoparticulate semiconductor as light absorber. The idea of coupling two nm-sized semiconductors to improve charge separation by inter-particle electron transfer was developed over the past two decades. Thus, it was shown that in a mixed TiO_2/CdS particle system, prior to semiconductor–electrolyte charge transfer, electrons that were photogenerated in the lower band gap CdS, were transferred to the TiO_2 while the holes remained in the CdS [2]. This type of work was gradually extended to other coupled semiconductor systems with increasing emphasis on the DSSC, where the absorbing semiconductor took the place of the dye. Most studies have been on CdS [3,4], CdSe [5–7] and PbS [3,8–10]. Other semiconductors have been deposited on porous, high band gap oxides for use as solar cells, including CdTe [11,12], $CuInS_2$ [13,14], $Cu_{1.8}S$ [15], Se [16], InP [17] and FeS_2 [18,19]. As is the case with many other semiconductor systems, post-preparation annealing often improves device performance [7].

The conceptual advantage of these nano-composite solar cells over most other types is that because of the high interfacial area between the absorber and the electron and hole conductors, electron–hole pairs are always generated close to a charge separating interface. In this case, carrier diffusion length requirements are relaxed in contrast to what is the case for conventional p–n junction cells. Therefore, the quality requirements for the absorber material are significantly lower than for normal p–n junction cells.

In depositing the absorbing semiconductor it is important that the absorber is deposited throughout the porous oxide layer, which is usually several microns thick. This condition requires a method that allows infiltration of the reactants into the pores of the oxide. Solution deposition methods are ideal for this purpose. While simple alternate dips of the porous oxide film into solutions of the anion and cation (e.g., Na_2**S** and **Pb**Ac_2) have

* Corresponding author. Tel.: +972 8 9342076; fax: +972 8 9344137.
E-mail address: gary.hodes@weizmann.ac.il (G. Hodes).
[1] These authors contributed equally to the work.
[2] Present address: Debye Institute, University of Utrecht, P.O. Box 80000, 3508 TA Utrecht, The Netherlands.

1010-6030/$ – see front matter © 2006 Elsevier B.V. All rights reserved.
doi:10.1016/j.jphotochem.2005.12.012

been used, chemical bath deposition (CBD) [20] is probably the most common solution method used. However, deposits from CBD can vary considerably depending on the deposition parameters. In particular, the nanocrystal size depends strongly on the deposition parameters [20].

In this paper we describe how the performance of photoelectrochemical cells based on CdSe- and CdS-sensitized porous TiO_2 depends on the CBD CdSe deposition conditions. In particular, we show that:

- the mechanism of the deposition, which can be controlled, is important in determining the cell performance,
- illumination during deposition increases the deposition rate greatly,
- a pre-deposited layer of CdS prior to CdSe deposition also improves the cell performance.

Reasons are suggested to explain these performance-deposition parameter dependences.

2. Experimental

2.1. Sample preparation

Commercially available P25 TiO_2 powder (ca. 75% anatase; 25% rutile) was mixed with ethanol [21] to make a paste, which is used to prepare the mesoporous electrode. The resulting paste was applied with a glass rod onto a fluorine-doped-tin oxide (FTO) coated glass substrate (typical resistivity is ∼8 Ω/sq, Pilkington Inc.) using Scotch tape as a spacer and frame (the doctor-blade method). These films were dried in air for ca. 15 min to remove excess solvent, after which they were sintered in ambient conditions at 250 °C for 45 min followed by another 45 min at 450 °C. Typical film thickness was 6–10 μm as determined by a thickness profilometer. SEM images (not shown) reveal a highly porous network with a typical crystal size of 20–30 nm.

In one set of experiments (clearly specified below), a ZnO layer was deposited on the TiO_2. This was carried out by dipping the TiO_2 film in 0.05 M aqueous zinc acetate for 3 h, followed by annealing at 300 °C in air for 2 h. This was repeated six more times. While the resulting ZnO was not characterized, this treatment was found, by optimization, to give improved fill factors.

CdS was deposited from the common NH_3 bath [22] with a solution composition of 20 mM $CdCl_2$, 66 mM NH_4Cl, 140 mM thiourea and 0.23 M ammonia with a final pH ca. 9.5. The deposition was carried out at room temperature and in normal room light.

CdSe was deposited by CBD using nitriloacetate as a complex and selenosulphate as Se source [20], although certain modifications were employed to ensure that the adsorber layer was deposited throughout the porous network. In brief, an aqueous solution of $CdSO_4$, potassium nitrilotriacetate ($N(CH_2COOK)_3$, referred to in this paper as NTA, and sodium selenosulphate (Na_2SeSO_3, prepared by refluxing 0.2 M Se powder with 0.5 M Na_2SO_3 at ca. 80 °C for several hours) were mixed to give a final composition of 80 mM of $CdSO_4$, 80 mM of Na_2SeSO_3 and 90 mM or 160 mM of NTA.

- Use of 90 mM NTA at a pH of ∼9.5, adjusted with KOH, resulted in a cluster mechanism deposition. In that case deposition occurs via selenization of $Cd(OH)_2$ colloids.
- Use of 160 mM NTA at a pH between 7.5 and 8.0, conditions under which no $Cd(OH)_2$ phase is present, led to deposition by an ion-by-ion mechanism.

Deposition was carried out at room temperature under normal fluorescent room lighting. Any variation to this procedure will be specifically specified where it occurs.

Some experiments were carried out by treating the CdS-coated TiO_2 with selenosulphate solution (one volume of the above mentioned 0.2 M Se + 0.5 M Na_2SO_3 solution diluted with two volumes of water). This is referred to in the text as selenosulphate conversion.

2.2. Characterization techniques

Optical transmission spectra were measured on a JASCO V-570 UV–vis–IR spectrophotometer fitted with an integrating sphere.

XRD measurements ($\theta-2\theta$) were made on a Rigaku RU-200B Rotaflex powder diffractometer using Cu Kα radiation. Crystal size was measured from XRD peak broadening using the Scherrer equation. The size measured by XRD was found to correspond closely with that measured by direct TEM imaging for these films [20].

IPCE (incident photon to current conversion efficiency) measurements were performed using a setup including a 300 W Xe arc lamp and monochromator (Oriel Cornerstone 1/4 m). The quantum efficiency was calculated using a standard Si photodiode (Hamamatsu Photonics).

I–V measurements were performed in three-electrode configuration, using a Wenking MP87 potentiostat, Keithley 230 programmable voltage source, Keithley 195A digital multimeter and Osram HLX 64634 Xenophot 15 V, 150 W tungsten–halogen lamp with transformer as the white light

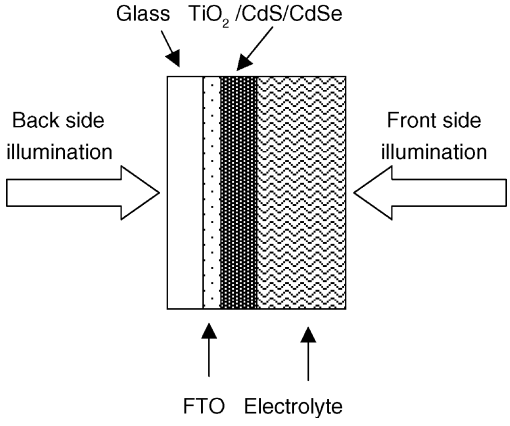

Scheme 1. Schematic diagram of the photoelectrochemical cell configuration used to measure the photovoltaic response of the nanocomposite films, showing back and front side illumination.

source. The intensity was set to ∼1 sun (set by measuring the short circuit currents of occasional cells outside in a bright day and setting the lamp to give the same current). Polysulphide electrolyte (1 M Na_2S, 0.1 M S and 0.1 M NaOH) was used for both *I–V* and IPCE measurements. The redox couple, electrolyte and concentrations were chosen both for optimum cell performance and stability for repetitive measurements. Measurements were performed with backside illumination, i.e., illumination through the glass substrate side (as shown in Scheme 1), unless specified otherwise.

SEM (scanning electron microscopy) measurements were performed with a SUPRA 55VP LEO microscope.

3. Results and discussion

3.1. CdSe deposition directly on TiO_2

CBD deposition of CdSe can occur by two fundamentally different mechanisms: ion-by-ion and cluster deposition [20]. As it is likely that the structure and some of the other properties of the TiO_2/CdSe composite will be affected by the deposition mechanism, we deliberately chose conditions where deposition occurred via one or the other mechanism. Illumination of the film during CdSe deposition accelerated the rate of deposition for both mechanisms compared with deposition in the dark for, but without any obvious effect on the photoelectrochemical performance. Illumination was previously found to increase the rate of deposition and sometimes also the nature of the deposit in CBD. The latter effect was ascribed to the occurrence of photoelectrochemical deposition in parallel with chemical deposition [23–26]. Samples described below were deposited under normal fluorescent room lighting. Stronger illumination, e.g., in direct sunlight, resulted in preferential deposition near the illuminated surface. The resulting inhomogeneity throughout the thickness of the film caused by strong illumination decreased the overall photoelectrochemical performance of the cell.

SEM cross-sectional imaging with electron-dispersive X-ray fluorescence specrtroscopy (EDS) analyses showed that the distribution of Cd and Se was essentially homogeneous throughout the thickness of the porous TiO_2 film for both mechanisms. This result was expected for ion-by-ion deposition but less so for the cluster deposition. For the latter it was thought that the initial $Cd(OH)_2$ colloids might be too large to penetrate the porous network.

There was also no difference in the photocurrent–voltage behaviour of electrodes made using the two different deposition techniques. Typical *I–V* plots for such electrodes are shown in Figs. 1 and 2.

3.2. CdS deposition on TiO_2

CdS is deposited on the TiO_2 much more readily than is CdSe. XRD of the CdS-on-TiO_2 showed the cubic (sphalerite) phase of CdS with an average particle size, determined from the peak broadening, of ca. 3.5 nm. EDS analysis of the deposit showed a large Cd excess (Cd:S ratio ≈5). Based on the mode of deposition of the CdS, it is expected that this excess is due to deposition of $Cd(OH)_2$ which is not removed by gentle rinsing.

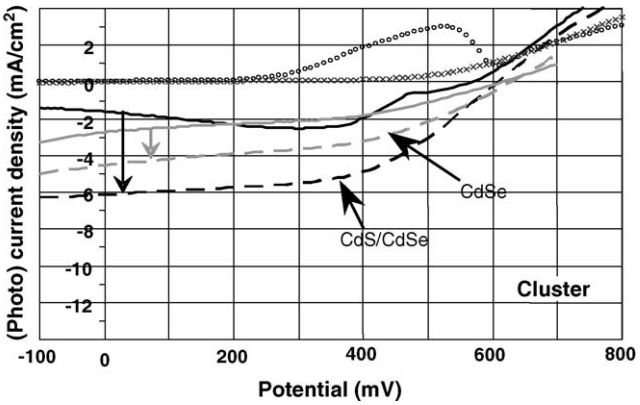

Fig. 1. (Photo)current–(photo)voltage measurements of a cluster-deposited CdSe film on TiO_2 and on CdS-coated TiO_2 (AM1 equivalent illumination as described in Section 2). The vertical arrows designate the change in characteristics from the initial scan to the stable electrode after several scans. Dark curves: crosses—CdSe; diamonds—CdS/CdSe.

3.3. CdSe deposition on CdS/TiO_2

Deposition of CdSe onto the TiO_2/CdS films by either cluster or ion-by-ion reactions is considerably faster than the same deposition on bare TiO_2. We ascribe this to pre-adsorbed/deposited $Cd(OH)_2$ or to the presence of a highly non-stoichiometric CdS layer. As with CdSe deposition directly onto TiO_2, illumination (room light) increases the deposition rate even further, but has no major effect on the final photoelectrochemical performance in comparison to depositions done in absolute darkness. In both cases, whether deposited by ion-by-ion or by cluster mechanisms, Cd and Se are found more or less homogeneously throughout the TiO_2 film, with a slightly stronger decrease in Se toward the FTO substrate than in the S or Cd as seen from the EDS data in Fig. 3.

One difference between the two types of films is the broad peak in the dark *I–V* of the CdS/CdSe sample (open circles,

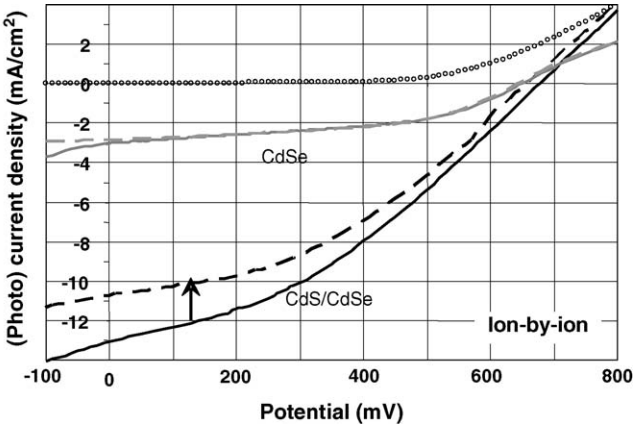

Fig. 2. As Fig. 1 but for ion-by-ion-deposited CdSe. The CdSe on TiO_2 sample was stable from the first scan. All the dark curves were similar and are depicted as a single curve. The characteristics of the stabilized cell were: J_{SC} = 10.5 mA cm^{-2}; V_{OC} = 660 mV; FF = 39.5% giving an efficiency of 2.8%.

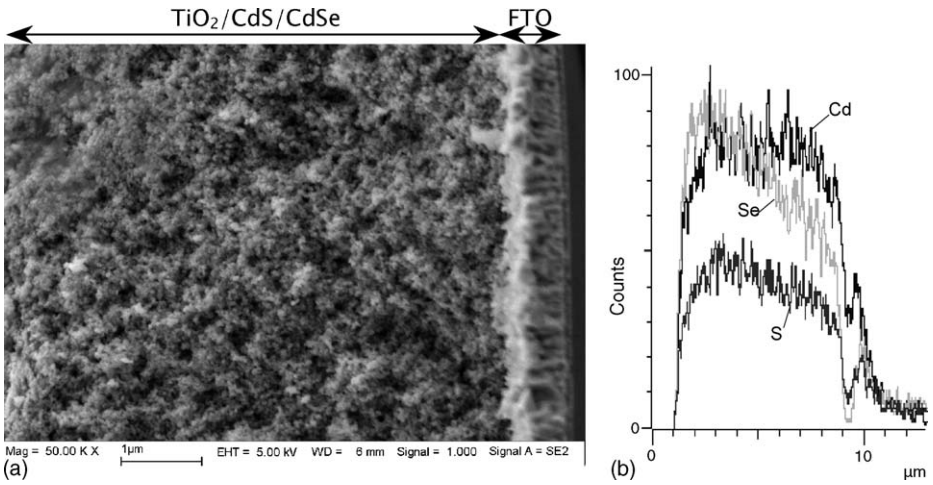

Fig. 3. (a) Cross-section SEM image of a standard cell (ion-by-ion TiO_2/CdS/CdSe); (b) elemental distribution (uncorrected raw data), measured by EDS, of Cd, Se and S throughout the thickness of the film. The front surface of the film is at ca. 1 μm and the SnO_2 interface at ca. 9 μm.

Fig. 1), which is seen for all cluster-deposited films during the first *I–V* scan. This peak, which disappears after the first scan, is not at all observed for any of the other types of samples, i.e., CdSe—whether cluster or ion-by-ion—without CdS; ion-by-ion CdSe on TiO_2/CdS; TiO_2/CdS. XPS analyses show S in reduced form (due to S/Se exchange [27]) in the cluster CdSe on TiO_2/CdS after cell operation in the polysulphide electrolyte, but no S in the equivalent ion-by-ion CdSe on TiO_2/CdS cells. It appears that the peak is due to an anodization reaction in the polysulphide solution.

There is also a clear difference in the photoelectrochemical behaviour of the resulting photoelectrodes, depending on the CdSe deposition mechanism. Short-circuit currents (I_{SC}) are considerably higher with ion-by-ion deposition (Fig. 2) than with cluster deposition (Fig. 1). Ion-by-ion deposition is known to give larger crystallite sizes than the cluster mechanism [20]. This is reflected in the transmission spectra of the films (Fig. 4), which are found to be red-shifted by ca. 50 nm compared to the cluster ones, resulting in larger photocurrents, all other factors being equal. We were unable to measure the crystallite size of the CdSe layers by XRD for these samples using the main (1 1 1) peak of (cubic) CdSe since the presence of the TiO_2 made the CdSe peak width impossible to estimate. However, using the smaller (2 2 0) CdSe peak at $2\theta = 42^\circ$, and correcting for the partially overlapping rutile peaks, a rough estimation could be made. The crystal size using this method was found to be ca. 5 nm for both mechanisms (this size is expected for the cluster mechanism but a larger size of at least 8 nm is expected for the ion-by-ion deposition [20]. Neither could we estimate the crystal size reliably from the optical spectra, since the shapes of the spectra resembled to some extent those of films electrodeposited from selenosulphate solutions, which do not follow a simple direct band gap behaviour [28]. This, in itself, is evidence for photoelectrochemical deposition as described above. Based on the optical spectra in Fig. 4, and the known dependence of CBD CdSe band gap on crystal size [20,29] we can estimate an upper limit for the crystal sizes, assuming a direct band gap behaviour, of 8 nm for the ion-by-ion deposition and 4.7 nm for the cluster deposition. Based on our knowledge of electrodeposited films from similar solutions, it is likely that the crystal size in ion-by-ion deposits is ca. 5 nm as suggested by the XRD data, and that close contact between neighbouring crystals (or possibly between the CdSe and TiO_2) reduces the degree of size quantization [28].

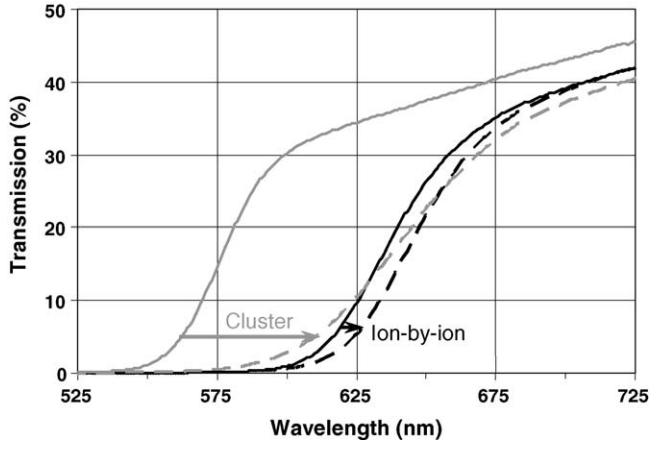

Fig. 4. Transmission spectra of a cluster-deposited CdSe (gray curves) and an ion-by-ion-deposited CdSe (black curves) on TiO_2/CdS. The beginning of the horizontal arrows shows the as-deposited films and the end shows the films after several *I–V* scans.

It may be argued that the $Cd(OH)_2$ which we believe to be present in the CdS-coated TiO_2 would result in a cluster deposition, even if a solution which normally results in an ion-by-ion deposition is used. This argument would be supported by the apparently small crystal size (ca. 5 nm estimated from XRD) of the ion-by-ion CdSe. However, the difference between the cluster mechanism deposition solution and that which proceeds by the ion-by-ion mechanism is the presence of enough complex (NTA) in the latter to prevent formation of $Cd(OH)_2$. This means that the ion-by-ion deposition solution should dissolve at least most of the $Cd(OH)_2$ in the porous layer in contrast to the cluster deposition solution. This is confirmed by EDS analyses which

show a large decrease in the Cd:(S + Se) ratio, from ca. 5 for the CdS/TiO_2 film to ca. 1.6 after 15 min of CdSe deposition, when the reaction is still in the early stages and the Se:S ratio is 0.6 compared to 3.5 at the end of the deposition (3 h, when the Cd:Se:S ratio is 1:0.87:0.25 measured by EDS at the front surface of the film). This means that much, but not all, of the $Cd(OH)_2$ has been removed by the deposition solution.

The remaining $Cd(OH)_2$ will eventually be converted to small crystal size CdSe by the selenosulphate (see Section 3.4). This might offer a partial explanation for the apparent small crystal size of the ion-by-ion deposits. However, we should still see a narrower XRD peak riding on the broader one due to the $Cd(OH)_2$-derived CdSe and this is not the case. It is possible that the restricted space in which the CdSe is deposited limits the crystal size. Another possibility is that the ion-by-ion deposition solution removes $Cd(OH)_2$ which is not directly bound to the TiO_2 leaving more strongly bound $Cd(OH)_2$ The resulting CdSe is also expected to be more strongly bound to the TiO_2, reflected in better electron transfer from the CdSe to the TiO_2.

After operation in the polysulphide solution, I_{SC} initially increases for the cluster-deposited films, at times by a factor of 2 or even more (Fig. 1) but decreases 10–20% for the ion-by-ion deposited films during the first few scans (Fig. 2) and then stabilizes. The increase for the cluster-deposited films is accompanied by a visible darkening of the films in the polysulphide electrolyte. We ascribe this to crystallite growth of these nanocrystalline CdSe films, which we find to occur in alkaline solution. XRD, in spite of its limited reliability, does show a clear narrowing of the (2 2 0) peak for the ion-by-ion samples, equivalent to a crystal size of ca. 8 nm after operation in polysulphide. For cluster mechanism samples, we obtained a very rough estimate of ~7 nm crystal size. It must be mentioned here, that after brief polysulphide treatment accompanied with illumination which results in darkening just as after *I–V* measurement, the initially poorly adhering samples peeled off as flakes from the FTO substrate completely. For this reason, we focused on the ion-by-ion-deposited films where such peeling does not occur.

This poorer adherence of the cluster-deposited films may explain their poorer performance compared to the ion-by-ion films: poor adherence of the CdSe/TiO_2 to the FTO, even if not manifested by visible peeling, is expected to cause a reduction in the photocurrent. However, other possibilities to explain the difference in photoelectrochemical performance should not be ignored, particularly in view of the lack of correlation between the apparent crystal size of the ion-by-ion films and their optical spectra. This could be explained by closer packing of the crystals compared to the cluster deposits leading to charge overlap and reduction of size quantization as suggested above. Such closer packing of the CdSe could also improve the photoelectrochemical behaviour. As discussed earlier, loss of quantization and improved photoelectrochemical behaviour might also be connected with stronger binding of the CdSe to the TiO_2.

3.4. Selenosulphate conversion

Treating the TiO_2/CdS samples with an aqueous selenosulphate solution results in the conversion of much of the

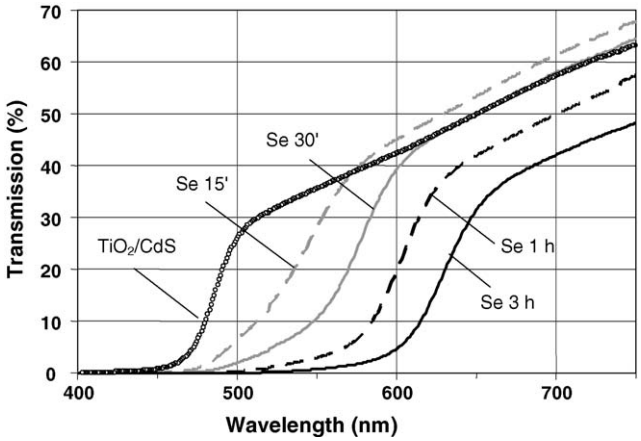

Fig. 5. Transmission spectra of a CdS-on-TiO_2 film (left spectrum) and the spectra after various immersion times (labeled in the figure) in selenosulfate solution.

CdS/$Cd(OH)_2$ deposit into CdSe. This can be seen from the changes in transmission spectra of CdS-coated TiO_2 as a function of selenosulphate treatment time (Fig. 5). It is likely that $Cd(OH)_2$ reacts with selenosulphate to form CdSe, which is the main process in the cluster mechanism of CdSe deposition by CBD. In support of this expectation, if the CdS/$Cd(OH)_2$ coated TiO_2 is treated with K_3NTA prior to selenosulphate treatment, no CdSe forms. This is because the K_3NTA dissolves any free $Cd(OH)_2$. In contrast, if the CdS/$Cd(OH)_2$-coated TiO_2 is treated with $CdCl_2$ solution, the rate of growth of CdSe by subsequent selenosulphate treatment is increased.

Use of selenosulphate to convert a $Cd(OH)_2$ deposit to CdSe has the potential advantage over the other methods that the original CdS/$Cd(OH)_2$ deposition limits the amount of CdSe that can be formed. As a result no additional CdSe (or $Cd(OH)_2$) is formed which might block the pores of the films. The I-V behaviour of these films, an example of which is shown in Fig. 6, is respectable although inferior to ion-by-ion samples .

The in situ selenization method can be compared to that, used to convert a $In(OH)_xS_y$ layer deposited by CBD on porous

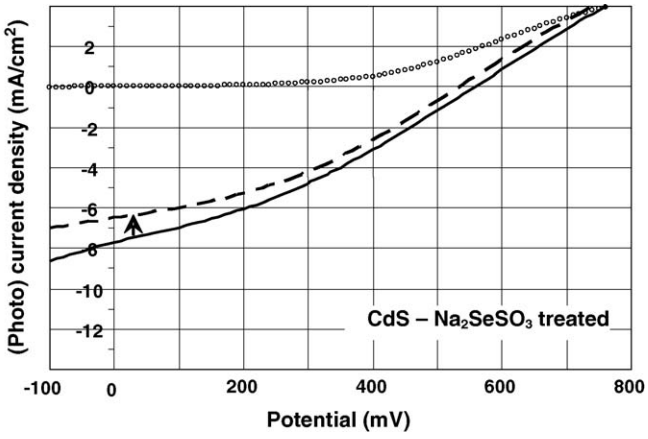

Fig. 6. (Photo)current–(photo)voltage measurements of a selenosulphate-treated (for 3 h) CdS-on-TiO_2 electrode. Solid line: first scan. Broken line: final (stabilized) scan.

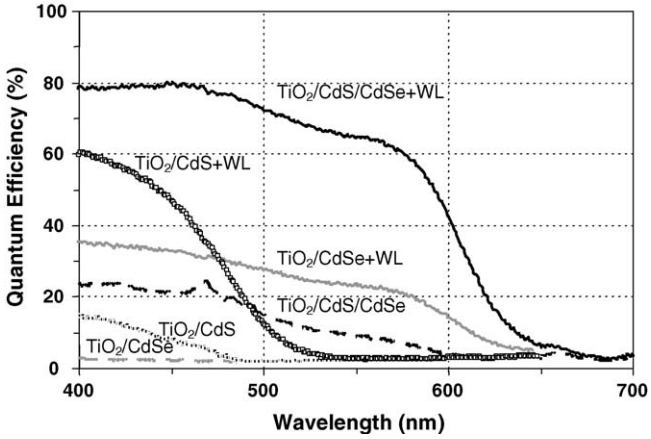

Fig. 7. Spectral response (external quantum efficiency) of three different photoelectrodes (ion-by-ion-deposited CdSe, CdS and CdS/CdSe-on-TiO_2). Each spectrum is given in the presence (+WL) and absence of white light illumination (ca. 60% of AM 1.5).

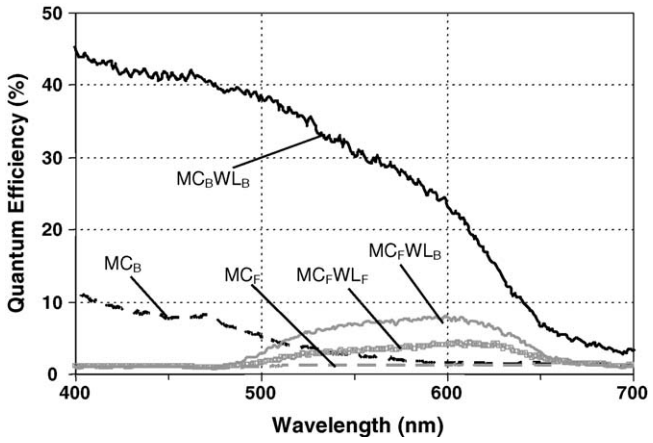

Fig. 8. Spectral response for a ion-by-ion-deposited CdSe on TiO_2/CdS photoelectrode with different illumination configurations. MC refers to monochromatic illumination while WL refers to the while light bias. The subscripts "F" and "B" designate front side and backside illumination, respectively.

TiO_2 by treating it with Pb^{2+} (cation exchange instead of anion exchange) [30]. The resulting layer contained some PbS. In that case, the short circuit current of the resulting photoelectrochemical cell was less and the open circuit voltage more than for an electrode made by simple dipping.[1]

3.5. Spectral response of the photocurrent

All the films show a pronounced enhancement of quantum efficiency if white light is added to the chopped monochromatic light (Fig. 7). The enhancement varies from 3 to 15 times and can be attributed to trap filling, which leads to better electron transport in the overall composite film.

White light bias also appears to give a large red shift (typically 50 nm) and a sharpening of the onset of the spectra with white light for both TiO_2/CdS and TiO_2/CdS/CdSe. However, this apparent red shift upon white light illumination is actually seen to be a very gradual increase of a low photocurrent with decreasing wavelength *at the same onset as for white light illumination,* followed by a sharper photocurrent increase at a shorter wavelength (Fig. 9). Since this true onset correlates with the onset of absorption in transmission measurements, the apparent red shift in the photocurrent spectra with white light means that the white light increases the collection efficiency near the absorption onset. To explain this phenomenon, we discuss first how the locus of the light absorption influences the collection efficiency.

Very large differences in the spectral response are observed, depending on whether the cell is illuminated from the backside (BS), the usual configuration in this work, or from the front side (FS). Figs. 8 and 9, the latter with an expanded quantum efficiency scale, show that for FS illumination, the charge collection efficiency is always much lower than for BS illumination. Also for FS illumination white light increases the current several-fold. FS illumination results in a fairly narrow spectral response peak at ca. 610 nm, something that is clearest seen with white light. The drop in current at short wavelengths is not due to light absorption by the polysulphide solution because that solution does not absorb near 600 nm. Rather, the difference between FS and BS illumination is that in the FS case, light is absorbed far from the substrate, which is where the electron–hole pairs are generated, while for BS illumination electron–hole generation is maximum close to the substrate (Scheme 2). The fact that we see the peak in the spectral response can, therefore, be explained by a short effective diffusion length of electrons in the TiO_2, much less than in the standard DSSC, where electrons can efficiently cross the entire ca. 10 μm thickness of the porous TiO_2 layer. The short diffusion length must be due to strong recombination, the source of which may be re-injection of electrons from the TiO_2 back into the electrolyte or possibly into the CdS/CdSe. While the conduction band of CdS (and to a lesser extent, CdSe) is normally higher than that of the TiO_2,

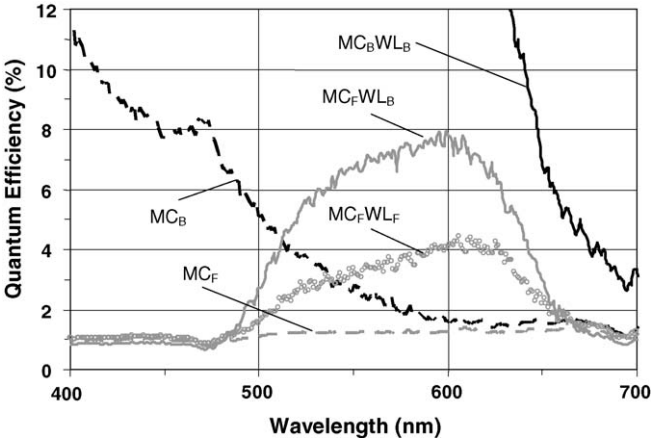

Fig. 9. As Fig. 8 but with an expanded quantum efficiency scale.

[1] The $In(OH)_xS_y$ layer did improve the overall performance, including the current, of a solid state cell using $CuInS_2$ as absorber and hole conductor. Electron–hole recombination was shown to be decreased by the interfacial $In(OH)_xS_y$ layer) [30].

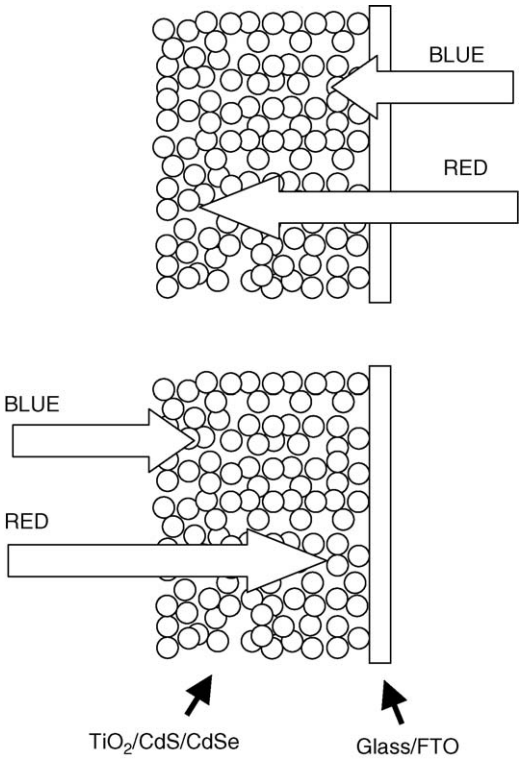

Scheme 2. Schematic diagram indicating the relative loci of light absorption in the porous layer depending on direction of illumination and wavelength of light. While both red and blue light are absorbed stronger at the illuminated side of the film than farther into the film, the red light penetrates further into the film than does the blue light.

the conduction band lineups are not so clear in the present case because of the high pH, which will shift the TiO_2 bands negative to a greater extent than any corresponding shifts of the CdS(e). The recombination cannot be due to recombination of electrons and holes in the CdS/CdSe since, if that was the major loss process, the quantum efficiencies for BS illumination would also be low.

Why are electrons, after their injection from CdS/CdSe into the TiO_2 so much more readily re-injected into the electrolyte than is the case for the standard DSSC? The most logical difference is in the nature of the electrolyte, polysulphide instead of polyiodide (ferro/ferricyanide gave much poorer results than the polysulphide). We could not use the polyiodide electrolyte that is used in the DSSC since CdSe is both photoelectrochemically and chemically unstable in this electrolyte.

If we are correct in assuming that the photocurrent, and, therefore, the photovoltage is limited by back injection of electrons from the TiO_2 to the electrolyte, then introducing a tunnel barrier at the adsorber–TiO_2 interface which has been shown to reduce recombination in the DSSC [31,32], may be beneficial. Of course, such a layer, if too thick, will reduce current since it will reduce the efficiency of electron transfer from CdSe(S) to TiO_2. In preliminary experiments in this direction we found that coating TiO_2 with ZnO (as described in Section 2) did reduce the photocurrent somewhat, although the fill factor increased which compensated most of the decrease.

We can now suggest a cause for the apparent red-shift of the photocurrent if white light is added, viz. the poor collection efficiency for electrons that are injected far from the substrate. From the transmission spectrum of the standard sample (Fig. 4), we see that near the absorption onset much of the light passes through the film and much of what is absorbed, will be absorbed far from the substrate. White light illumination, particularly from the backside, greatly increases the collection efficiency for monochromatic illumination near the absorption edge for both BS and FS illumination. This increase can be explained, as was the overall increase in collection efficiency for BS cells under white light illumination above, by better conductivity of the film due to trap filling. In other words, the increased conductivity of the film due to white light results in a larger improvement for monochromatically photons, the farther they are absorbed from the substrate, i.e., photons with an energy only slightly larger than the band gap.

For the FS cell, where even the near-band gap light is absorbed relatively far from the substrate (e.g., from Fig. 4, it can be calculated that only a few percent of the 600 nm illumination is absorbed within 1 or 2 μm from the substrate), the improved conductivity due to white light illumination can increase the near-band gap illuminated cell, but is not sufficient to allow collection from higher energy photons absorbed very far from the substrate (hence the peak in the response—Fig. 7). A much thinner TiO_2 layer would be expected to perform better under FS illumination.

3.6. Role of the CdS or $Cd(OH)_2$

Probably the main question to be answered is: why does a CdS/$Cd(OH)_2$ prelayer improve the performance so much? In the following we provide some guidelines and possibilities to answer this.

Simplistic considerations of the CdS/CdSe band lineup, taking into account size quantization and complete depletion of the nanocrystals lead to the expectation that the CdSe conduction band (more correctly, level) will be a little lower than that of the CdS while the CdSe valence band will be possibly slightly higher than that of the CdS. This would imply that photogenerated electrons (to a smaller extent, also holes) would be localized in the CdSe and that electron transfer from the CdSe to the CdS would be impeded relative to direct transfer from CdSe to TiO_2. However, such a conclusion would be highly oversimplified for a number of reasons. One is that, assuming that holes are readily transferred from the CdSe to the polysulphide electrolyte (as is often accepted in this system), then charging of the CdSe with electrons could lift the CdSe conduction band above that of the CdS. Another is the effect of the high pH of the electrolyte on the band edges described above. Thirdly, changes of the assumed complete depletion (i.e. midgap Fermi levels) by charge generation means it only requires very small perturbations to shift these levels by some tenths of an eV, and such shifts could dramatically change the band offsets, which are not expected to be very large to begin with.

It may also be oversimplified to assume that the CdSe is connected via the CdS to the TiO_2. It is possible that the active

CdSe forms from the excess Cd remaining after CdS deposition directly on the TiO_2. In this case, the better performance of the cell containing CdS could be due either to the different nature of the CdSe (or TiO_2/CdSe junction) deposited by this manner or to some passivation effect of the CdS on the TiO_2 surface rather than connected with energy level alignments.

A recent study of photoelectrochemical cells using PbS dip-coated onto porous TiO_2 showed that coating the PbS with a further coat of CdS (or CdS followed by ZnS) approximately doubles the photocurrent [33]. They explain this improvement as caused by cascading of electrons from CdS to PbS to TiO_2. This appears to be an unlikely explanation: if this were the case, then improvement would be seen only for wavelengths where CdS absorbs, while in fact, the improvement extends over the entire spectral range of the PbS absorption. A more likely explanation is that the CdS cap passivates the PbS with respect to electron–hole recombination. This would then increase the probability of electron injection into the TiO_2.

4. Conclusions

CdSe-sensitized porous TiO_2 photoelectrochemical cells were studied with emphasis on the mode of (chemical bath) deposition of the CdSe. Deposition of a $Cd(OH)_2$-rich CdS layer prior to CdSe deposition resulted in a major improvement in performance. Treatment of this CdS (Cd-rich) layer by selenosulphate instead of direct CdSe deposition resulted in performance only a little poorer than that obtained using CdSe deposition onto the CdS. CdSe deposited by an ion-by-ion process was found to give superior cell performance to that deposited by a cluster process. Illumination during the CdSe deposition increased the rate of deposition. Frontwall-illuminated cells were far inferior to backwall cells, and showed a narrow spectral range of photoactivity, indicating the high rate of recombination of electrons in the TiO_2. The chopped monochromatic spectral response was several times less than the same response when an additional constant white light source was used and this was explained by trap filling leading to better electron transport in the porous TiO_2. Stabilized solar efficiencies up to 2.8% were obtained in cells using a polysulphide electrolyte.

Acknowledgements

We thank Frank Lenzmann (ECN) for the TiO_2 paste and Hagai Cohen (WIS) for the XPS measurements. This research was supported in part by the Israel Science Foundation, the G.M.J. Schmidt Minerva Center for Supramolecular Chemistry and the PHOREMOST Network of Excellence. DC holds the Schaefer Chair in Energy Research.

References

[1] A. Hagfeldt, M. Gratzel, Chem. Rev. 95 (1995) 49–68.
[2] N. Serpone, E. Borgarello, M. Gratzel, J. Chem. Soc. Chem. Commun. (1984) 342–343.
[3] H. Weller, Ber. Bun. Gesellsch.: Phys. Chem. Chem. Phys. 95 (1991) 1361–1365.
[4] S. Hotchandani, P.V. Kamat, J. Phys. Chem. 96 (1992) 6834–6839.
[5] D. Liu, P.V. Kamat, J. Phys. Chem. 97 (1993) 10769–10773.
[6] C. Nasr, P.V. Kamat, S. Hotchandani, J. Electroanal. Chem. 420 (1997) 201–207.
[7] M.E. Rincon, A. Jimenez, A. Orihuela, G. Martinez, Sol. Energy Mater. Sol. Cells 70 (2001) 163–173.
[8] P. Hoyer, R. Konenkamp, Appl. Phys. Lett. 66 (1995) 349–351.
[9] S.M. Yang, Z.S. Wang, C.H. Huang, Syn. Metals 123 (2001) 267–272.
[10] R. Plass, S. Pelet, J. Krueger, M. Gratzel, U. Bach, J. Phys. Chem. B 106 (2002) 7578–7580.
[11] K. Ernst, R. Engelhardt, K. Ellmer, C. Kelch, H.J. Muffler, M.C. Lux-Steiner, R. Konenkamp, Thin Solid Films 387 (2001) 26–28.
[12] C. Levy-Clement, A. Katty, S. Bastide, F. Zenia, I. Mora, V. Munoz-Sanjose, Physica E 14 (2002) 229–232.
[13] I. Kaiser, K. Ernst, C.H. Fischer, R. Konenkamp, C. Rost, I. Sieber, M.C. Lux-Steiner, Sol. Energy Mater. Sol. Cells 67 (2001) 89–96.
[14] M. Nanu, J. Schoonman, A. Goossens, Adv. Funct. Mater. 15 (2005) 95–100.
[15] L. Reijnen, B. Meester, A. Goossens, J. Schoonman, Mater. Sci. Eng. C: Biomim. Supramol. Syst. 19 (2002) 311–314.
[16] K. Tennakone, G. Kumara, I.R.M. Kottegoda, V.P.S. Perera, G. Aponsu, J. Phys. D: Appl. Phys. 31 (1998) 2326–2330.
[17] A. Zaban, O.I. Micic, B.A. Gregg, A.J. Nozik, Langmuir 14 (1998) 3153–3156.
[18] A. Ennaoui, S. Fiechter, H. Tributsch, M. Giersig, R. Vogel, H. Weller, Electrochem. Soc. 139 (1992) 2514–2518.
[19] Y.C. Shen, H.H. Deng, J.H. Fang, Z.H. Lu, Colloid. Surf. A: Physicochem. Eng. Aspects 175 (2000) 135–140.
[20] S. Gorer, G. Hodes, J. Phys. Chem. 98 (1994) 5338–5346.
[21] B. O'Regan, F. Lenzmann, R. Muis, J. Wienke, Chem. Mater. 14 (2002) 5023–5029.
[22] R. Jayakrishnan, J.P. Nair, B.A. Kuruvilla, S.K. Kulkarni, R.K. Pandey, Semicond. Sci. Tech. 11 (1996) 116–123.
[23] P.K. Nair, V.M. Garcia, A.B. Hernandez, M.T.S. Nair, J. Phys. D: Appl. Phys. 24 (1991) 1466–1472.
[24] G. Hodes, Isr. J. Chem. 33 (1993) 95.
[25] S. Somasundaram, C.R. Chenthamarakshan, N.R. de Tacconi, Y. Ming, K. Rajeshwar, Chem. Mater. 16 (2004) 3846–3852.
[26] P. Nemec, D. Mikes, J. Rohovec, E. Uhlirova, F. Trojanek, P. Maly, Mater. Sci. Eng. B: Solid State Mater. Adv. Technol. 69 (2000) 500–504.
[27] D. Cahen, G. Hodes, J. Manassen, Electrochem. Soc. 125 (1978) 1623.
[28] G. Hodes, E. Grunbaum, Y. Feldman, S. Bastide, C. Levy-Clement, J. Electrochem. Soc. 152 (2005) G917.
[29] S.K. Sarkar, G. Hodes, J. Phys. Chem. B 109 (2005) 7214–7219.
[30] J. Wienke, M. Krunks, F. Lenzmann, Semicond. Sci. Technol. 18 (2003) 876–880.
[31] S.G. Chen, S. Chappel, Y. Diamant, A. Zaban, Chem. Mater. 13 (2001) 4629–4634.
[32] F. Lenzmann, M. Nanu, O. Kijatkina, A. Belaidi, Thin Solid Films 451–52 (2004) 639–643.
[33] S.M. Yang, C.H. Huang, J. Zhai, Z.S. Wang, J. Jiang, J. Mater. Chem. 12 (2002) 1459–1464.